

Analysis of the Performance of Ultrasonic Transducers

초음파 탐촉자의 성능 평가법

Yongrae Roh*

노 용 래*

ABSTRACT

A theoretical method to analyze ultrasonic transducer performance is developed and is applied to the design of a dual element transducer. The method can check both transmitting and receiving properties of a transducer, and can also reflect the diffraction effect of acoustic backscattering in both the frequency and time domains. In the time domain, distinct from the conventional method-inverse transform of frequency domain properties-, the method checks wave interferences at the interface of each material composing the transducer and calculates the transient response in a direct manner without relying on frequency domain results.

요 약

초음파 탐촉자 성능의 이론적 평가법을 개발해 이중소자 탐촉자에 적용하였다. 본 방법은 탐촉자의 발신, 회절, 수신 특성을 주파수, 시간 영역에서 평가할 수 있으며, 특히 시간영역에서는 통상 사용하는 역푸리에 변환법에 의존하지 않고 음파의 투과, 반사 특성을 고려해 파형을 직접 구할 수 있다.

I. Introduction

NDT is used, in manufacture, to ensure quality and, in service, mainly to ensure continued freedom from defects. Specific defects or the whole of a component giving concern may be assessed, to ensure fitness for purpose in conjunction with a fracture mechanics assessment. Ultrasonics is well suited to all these tasks, because it has the ability to detect defects and to determine their location and size. Piezoelectric ceramics are becoming increasingly important in ultrasonic transducer design.

*Research Institute of Industrial Science and Technology.

Because of its high electro-mechanical coupling, transducers made from these materials have excellent admittance and transmission characteristics. The operating frequency is generally in the low megacycle range, and, usually a thickness mode operation is employed. Main desired characteristics are a wide bandwidth which gives short echoes, a low transmission loss which gives good sensitivity, and a phase linearity over the operating bandwidth while ripple in the bandpass region is of a secondary importance.

Several theoretical methods for analyzing transducer performance have been reported in the literature. Most of them used the one dimensional theory developed by Mason⁽¹⁾ and extended by

Kossoff^[2], Sittig^[3], and others^[4]. With the help of well-developed electric circuit theories, the method can give a fairly good view of the transducer characteristics. However, transducer performance is difficult to evaluate by a frequency domain analysis only because transducers that give the broadest frequency characteristics do not necessarily have the best phase profile and pulse duration properties. Pulse waveforms can be determined by the Inverse Fourier Transform, but the computation time is too long for this approach to be of practical value in design. In addition, although the preceding references addressed the transient response of piezoelectric transducers, the generation and propagation of acoustic transients in the media of interest were totally ignored or treated in only an approximate manner. More specifically, only acoustic plane wave propagation was assumed. The effects of acoustic diffraction from planar radiators with specified wide bandwidth velocities has been a subject of interest. Rayleigh presented a retarded potential solution to the field problem in the form of surface integral, however, numerical results are not readily obtained from the solution.

This paper addresses the transmit/diffract/receive response of pulsed piezoelectric transducers. A systematic approach is presented in Sec.2 to develop a model of a transducer which clearly illustrates the effects of transducer dynamics, acoustic diffraction, and acoustic targets of interest on the performance of an ultrasonic thickness expander. The frequency domain approach is based on the viewpoint that the transducer can be represented as a lossy, three-port distributed parameter model following Mason. On the other hand, the time domain approach is based on analyses of the multiple interference of waves at each interface of transducer composing materials. It provides waveforms directly, permitting an easy evaluation

of sensitivity and response. Another advantage is that one can easily obtain a physical image of the behavior of the acoustic waves within the transducer. Section 3 describes results of the numerical analysis based on the idea. The algorithm described in Sec. 2 is a very general one. It can be employed for any type of transducers. However, Sec. 3 deals with a specific type of a transducer, a dual element transducer, which is of a particular interest to the author. Further work required to elaborate the method is outlined in the final section.

II. Approach

The basic problem of interest here is the development of an approach to evaluate the pulse echo response of a typical piezoelectric ultrasonic transducer. The configuration investigated is shown in Fig. 1. The transducer consists of a piezoceramic plate-for example, PZT-, and several matching layers on both the front and rear surfaces of the plate. Hereafter, the layers on the rear side will be called backing layers. The front matching layers also serve as an acoustic window to protect the piezoceramic from the radiation medium. In addition to the mechanical layers, an electrical network may

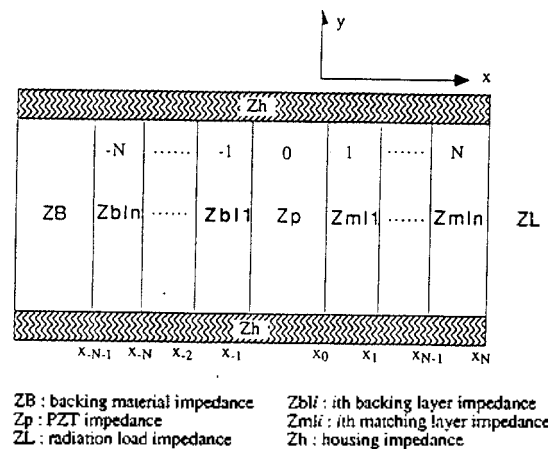


Fig. 1. Schematic structure of a typical piezoceramic ultrasonic transducer

be included at the electrical port for matching and shaping the response which results from the pulsed excitation of the transducer. All the layers are mounted in a housing.

For analyses of the transducer performance in the frequency domain, the entire assembly is represented by an equivalent circuit. The familiar three port distributed parameter Mason model is used for the present study as shown in Fig. 2. Material losses are readily included within the model via the use of complex material constants which lead to a complex wavenumber in the harmonic representation. The specific case of a transmitting transducer is represented by the modified circuit of Fig. 3-a. This model can be used to investigate not only the transducer performance but also the effect of changes in any sections of the circuit, i.e., changes in loading, number and kind of matching layers, mounting, piezoceramic and other materials.

In order to evaluate the pulse echo response, the transducer model must now be coupled to the response of the acoustic medium. The harmonic pressure $P(R, \omega)$ at an arbitrary point R from a radiator in the field can be related to the velocity

$V(\omega)$ of the radiator via the Rayleigh integral^[5] as

$$P(R, \omega) / V(\omega) = ikc \rho H(R, \omega) \tag{1}$$

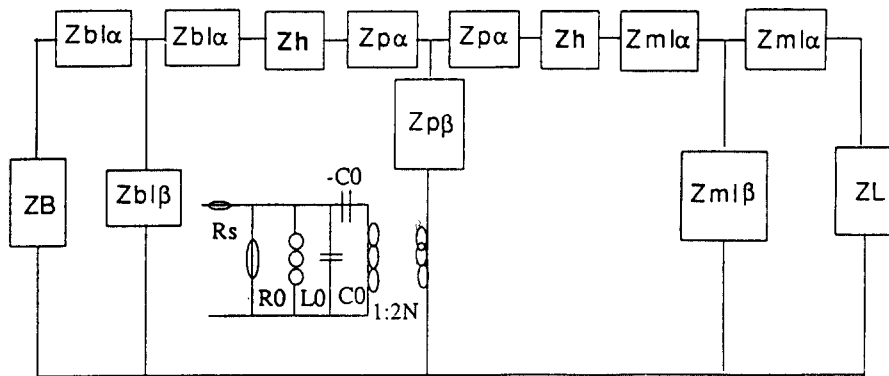
where

$$H(R, \omega) = \int \frac{e^{-ikR}}{2\pi R} ds$$

c is the sound velocity in the field, and ρ is the density of the field medium. It is implicit that the velocity be uniform over the surface of the radiator, i.e. the transducer, ideally baffled. Since the incident pressure $P(R, \omega)$ onto the target is the output of the transmitting transducer, it is considered to be known. The reflected pressure $P(R', \omega)$ at a distance R' from a small stationary target may thus be expressed as

$$\frac{P_s(R', \omega)}{P(R, \omega)} = S(\omega) \frac{e^{-ikR'}}{4\pi R'} \tag{2}$$

where $S(\omega)$ is a measure of the scattering strength of the target. The harmonic force which acts on



$Zx\alpha : i Zx \tan (a/2)$ k : wave number
 $Zx\beta : -i Zx / \sin(a/2)$ l : layer thickness
 $a : kl$ N : turning ratio of the piezoceramic

Fig. 2. Mason's equivalent circuit of the NDT transducer

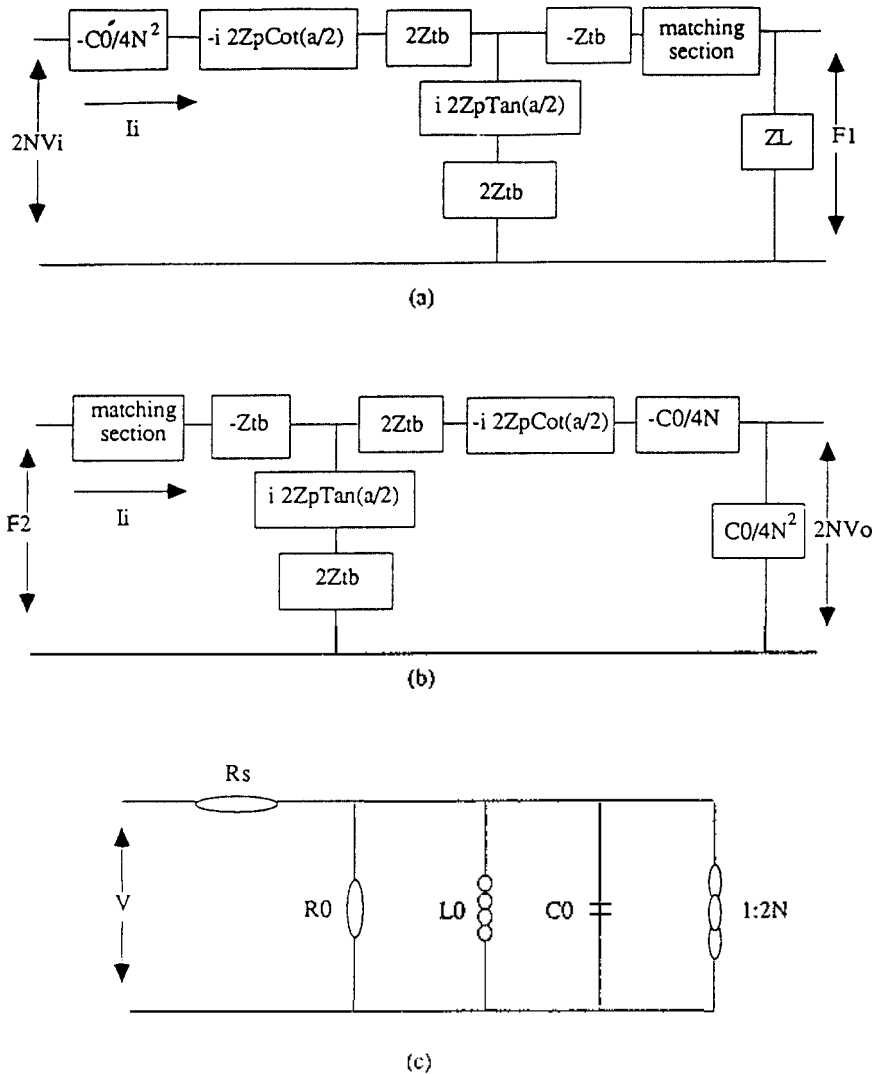


Fig. 3. Equivalent circuits of (a) transmitting and (b) receiving transducers. (c) is the matching electric circuits connected to (a) and (b). Z_{tb} is the equivalent impedance to the sum of backing material, backing layers, and housing. V_i is input voltage, V_o output voltage, F_1 transmitting force, and F_2 receiving force.

the transducer as a result of the acoustic backscattering process can be expressed as

$$F(\omega) = \int P_s(R', \omega) ds \quad (3)$$

where the rigid baffle effect is postponed to be considered in the analysis of receiving transducers. Here for the backscattering, R' is equal to R and

the returned force $F(\omega)$ to the receiving transducer is thus

$$F(\omega) / P(R, \omega) = H(R, \omega) S(\omega), \quad (4)$$

Therefore the transfer function of the acoustic backscattering is written as

$$G(R, \omega) = i k c_p S(\omega) H^2(R, \omega) \quad (5)$$

This property of the acoustic load is coupled to the response of the transmitting transducer, and is input to the receiving transducer. The voltage transfer properties of the receiving transducer can now be analyzed by the equivalent circuit shown in Fig. 3-b which is derived from the general circuit in Fig. 2. A single transducer can do the role of both the transmitting and receiving probes or separate transducers can do it depending on applications. The procedure so far can reveal the characteristics of the transducer of interest in the frequency domain, such as operating bandwidth, transduction loss, and phase profile.

Since the mathematical model of the equivalent transducer circuit is valid over the whole frequency spectrum, the transient response may be analyzed by the Inverse Fourier Transform. For the general case, including the effects of electrical terminations, the calculations are laborious. So instead of the indirect time-consuming task, a direct method is employed to characterize the transducer in the time domain. The application of a unit impulse voltage at time $t=0$ causes the piezoelectric vibrator to do piston-like movement in the thickness direction to generate four acoustic waves at both of its faces (up-going and down-going waves at each face) as noted A_1^+ , A_0^- , A_0^+ , and A_1^- in Fig. 4. When input voltage V_{in} is applied from a source, the force equilibrium equation at the PZT front face is derived from the constitutive equations of piezoelectricity⁽⁶⁾ as

$$(Z_p + Z_{b11}) v = e S V_{in}' / l_p \quad (6)$$

where v is the particle velocity at the interface, e is the piezoelectric constant, S is the interface area, V_{in}' is the input voltage which has passed

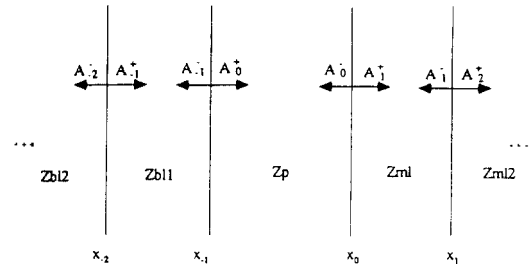


Fig. 4. Generation of four acoustic waves by the piezoelectric element (Z_p) and successive transmission and reflection of the waves at adjacent layer interfaces

through the electric tuning circuit, and l_p is the PZT plate thickness. A_1^+ is defined as the displacement amplitude of the up-going wave at the front face, and is related to the force equilibrium condition as

$$\begin{aligned} \rho_{b11} (-i\omega)^2 A_1^+ &= -Z_p v \\ &= -\frac{e S V_{in}'}{l_p} \frac{Z_p}{Z_p + Z_{b11}} \quad (7) \end{aligned}$$

Similar equations can be set up for the other three initial field amplitudes A_0^- , A_0^+ and A_1^- . The four acoustic waves generated at either face of the vibrator propagate through the transducer with repeated reflection and transmission at each of the boundaries between the impedance media. It is assumed that reflections from the back face of the backing material are absorbed within the backing material and do not return to the vibrator, and will thus be disregarded. When a medium consists of discrete layers of prescribed thickness and properties like this transducer, the reflection and transmission coefficients can be obtained in a systematic manner by just enforcing appropriate boundary conditions at each interface, continuity of the field and its normal derivative. Let A_i be the total wave amplitude in the i -th layer. At each interface of the layers, there is a reflected wave

and an incident wave. Thus

$$A_i(x) = A_i^+ e^{ik_i x} + A_i^- e^{-ik_i x} \quad (8)$$

The \pm superscripts denote waves traveling in the positive and negative thickness direction, respectively. A generalized reflection coefficient for any medium is defined as the ratio of the down-going field to the up-going field. Thus

$$\Gamma_i(x) = \frac{A_i^- e^{-ik_i x}}{A_i^+ e^{ik_i x}} = \frac{A_i^-}{A_i^+} e^{-2ik_i x} \quad (9)$$

and hence,

$$A_i = A_i^+ e^{ik_i x} (1 + \Gamma_i(x)) \quad (10)$$

If Z_i is the acoustic impedance of the i th layer, the total field impedance^[7] is defined as

$$X_i = Z_i \frac{1 + \Gamma_i}{1 - \Gamma_i} \quad (11)$$

which is complex and also position dependent. For the radiation load, X_1 is equal to Z_L . We start at the interface between the outer-most matching layer and load whose x coordinate is x_N as noted in Fig. 1. Choose a new origin at x_N and match the impedances at the origin and obtain

$$X_N(x=0) = X_L = Z_L. \quad (12)$$

Thus

$$\Gamma_N(0) = (Z_L - Z_N) / (Z_L + Z_N) \quad (13)$$

where Z_N is equal to Z_{\min} . A useful formula can be introduced to determine the reflection function

at a point x' if the reflection function at a point x is known,

$$\Gamma_i(x') = \Gamma_i(x) e^{-2ik_i(x' - x)} \quad (14)$$

From Eq. 13 and 14, the total field impedance can be obtained at $x = -d_N$, with respect to the origin at $x = x_N$. Here d_N is the thickness of the N th layer (outer-most matching layer). Thus

$$X_N(-d_N) = Z_N \frac{1 + \Gamma_N(0) e^{2ik_i d_N}}{1 - \Gamma_N(0) e^{2ik_i d_N}} \quad (15)$$

Now, the total field impedance at $x = x_{N-1}$ is matched with that of the second layer to the load. For the material in $x_{N-2} \leq x \leq x_{N-1}$, a new origin is chosen at $x = x_{N-1}$. The procedure can be repeated till we reach the wave generating surface, i.e. the surface of the piezoelectric ceramic. Hence

$$A_1(x) = A_1^+ e^{ik_1 x} (1 + \Gamma_1(0)) e^{-2ik_1 x} \quad (16)$$

The amplitude A_1^+ is that of the incident wave which is known from the Eq. 7. Now the continuity of the field across each interface is enforced and field amplitudes in all the other layers are determined. Once this routine is established, the wave amplitude penetrating into the load can be easily calculated by applying this algorithm to the four acoustic waves generated by the piezoceramic. The great advantage of this method is that only one unknown occurs in an equation at each step of the solution and large sets of simultaneous equations need not be solved. The impedance method is iterative and can even be implemented in a programmable calculator, whereas the Inverse Fourier Transform method should be done with a main computer.

Now the time domain transfer function of the

loading medium is calculated and applied to the acoustic waves. In a similar way as in the frequency domain, the pressure applied to the target is

$$p(R,t) = \frac{\rho}{2\pi R} \int \dot{v} ds \quad (17)$$

where v is the velocity on the surface of the outermost matching layer, which can be easily obtained from the above results. The field at the distance R' scattered by the small stationary target is

$$p_s(R',t) = \frac{s(t)}{4\pi R'} p(R,t) \quad (18)$$

The harmonic force which acts on the transducer as a result of the acoustic backscattering process ($R=R'$) can be expressed as

$$f = \int p_s(R,t) ds \quad (19)$$

This time domain property of the acoustic backscattering is convoluted with the transient response of the transmitting transducer and is reinput to the receiving transducer. The field reaching the piezoceramic and output voltage drop across it can be determined in the same fashion as before.

III. Numerical Results

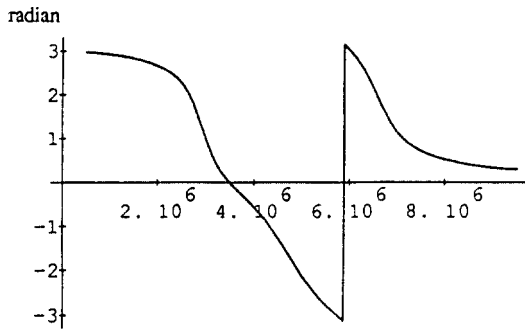
The method developed in Sec. 2 is a very general one. It can be applied to any type of transducers. In this section, as an example of the analysis with the algorithm, a specific type of transducers—a dual element transducer in which separate transmitting and receiving parts are contained in a single housing—is investigated, which is one of the most widely used types in steel

companies. The dual element transducer of the author's interest is made of RIST-developed PZT, one matching layer having the acoustic impedance of $\sqrt{Z_p Z_L}$, and one backing layer of $\sqrt{Z_p Z_B}$ following the rule of Goll^[14]. The transmitting and receiving parts share the same matching layer, backing layer, and backing material while each part has its own PZT element. For the electric tuner, only the transmitting part has an inductor, and the receiving part has none. The reason to have this unsymmetrical tuning circuit is to get the best trade-off between the maximum transduction efficiency and the minimum ringing in the LC circuit. Properties of the materials are shown in Table 1. The thickness of the backing and matching layers is chosen to be a quarter wavelength. The effect of electrodes and bonding layers between each material is ignored by assuming it is sufficiently thin. Acoustic losses in all materials are ignored.

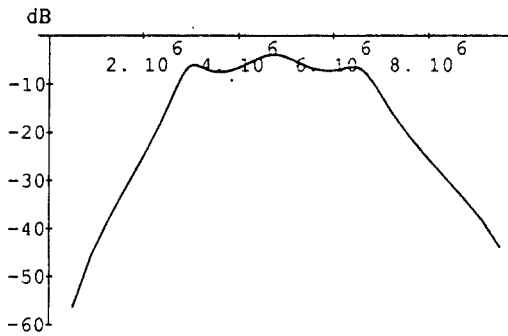
With the equivalent circuit of a transmitting transducer, the voltage transfer ratio(VTR) and phase variation is determined and is shown in Fig.

Table 1. Properties of the materials composing the ultrasonic transducer

	d_{33}	400pm/V
	h_{33}	18.0E8 V/m
	f_r (resonant freq.)	5.0 MHz
	C_0	2700 pF
PZT	sound velocity	4000m/s
	density	7800 kg/m ³
	N (turning ratio)	4.9
	thickness	0.4mm
	area	122mm ²
matching layer	acoustic impedance	6.8Mrayl
	acoustic impedance	9.7Mrayl
back layer	acoustic impedance	3.0Mrayl
	acoustic impedance	9.5Mrayl
back load	acoustic impedance	0.5mH
	inductor	
housing	acoustic impedance	
matching circuit	inductor	



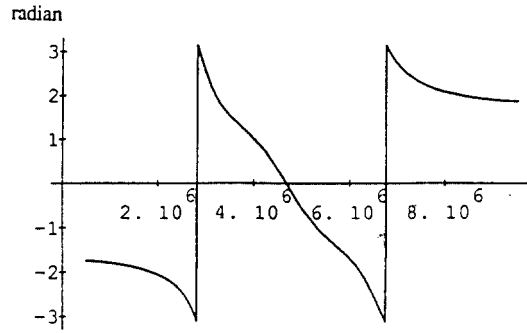
(a) phase spectrum



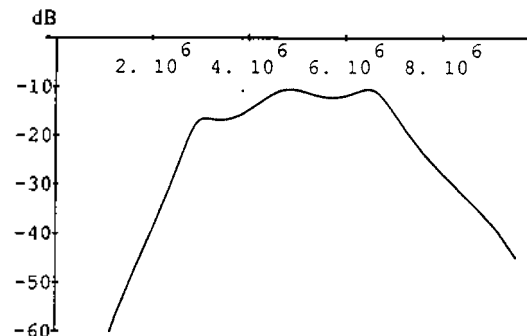
(b) power spectrum

Fig. 5. Performance of the transmitting transducer

5. 3dB bandwidth is about 76%. It has a fairly linear phase profile and flat VTR variation over the operating bandwidth. The transfer function $G(R,\omega)$ of the backscattering through a radiation medium, water, is calculated and applied to the wave generated by the transmitter. For the scattering strength, only monopole term is considered for simplicity by assuming an idealized point scattering. The target is located $\frac{2a^2}{\lambda}$ away from the transducer (a : equivalent transducer radius, λ : wavelength) to satisfy the far field condition safely. The distance $\frac{a^2}{\lambda}$ corresponds to the transition from near field to far field. For the target inside the transition region, higher order terms of scattering strength should also be included in the calculation. Figure 6 shows the power and phase variation of the wave after plying from the trans-



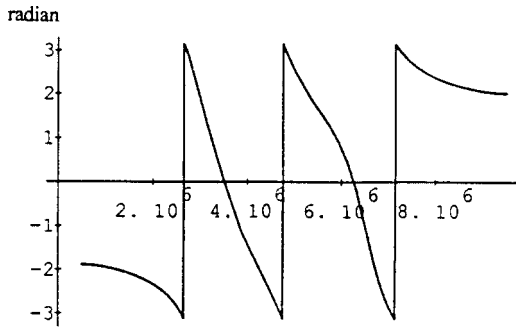
(a) phase spectrum



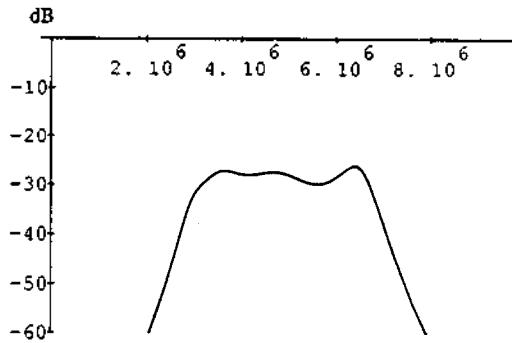
(b) power spectrum

Fig. 6. Transmitted signal after plying from the transmitting transducer to the target

ducer to the target. A dominant feature in many scattering phenomena is that high frequencies scatter much more than low frequencies, and the same situation is observed in the Fig. 6. The power spectrum looks a little bit larger than the author's initial guess. This is primarily because he assumes a complete total backscattering at the surface of the target and the absence of acoustic loss in the radiation medium. Now the returned signal is applied to the receiving transducer and the response of the receiving probe is analyzed with the help of the equivalent circuit in Fig. 3-b. The results are shown in Fig. 7. What they mean is an overall transmit / diffract / receive voltage transfer ratio and phase characteristics of the dual element transducer. For comparison, the overall transmit / receive responses of the transducer disregarding

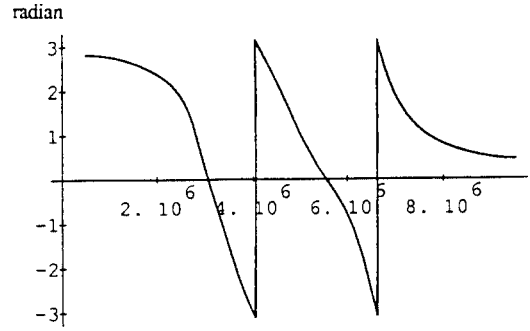


(a) phase spectrum

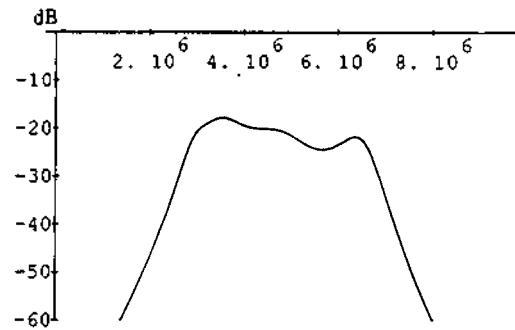


(b) power spectrum

Fig. 7. Overall performance of the dual element transducer with diffraction



(a) phase spectrum



(b) power spectrum

Fig. 8. Overall performance of the dual element transducer without diffraction

the effect of diffraction are shown in Fig. 8. The effect of diffraction on the performance of ultrasonic transducers is clearly demonstrated in the two figures, Fig. 7 and 8, especially in the high frequency range. Overall 6dB bandwidth remains almost the same, about 76%, but the transduction loss increases by about 6dB due to the diffraction. Linearity of the phase profile deteriorates, too.

In the time domain, the transmitted signal by the transducer is shown in Fig. 9. The driving waveform used here is a half cycle sine wave at the resonant frequency of the piezoceramic vibrator. In the figure, the horizontal axis denotes relative time values normalized with a time constant $(1/16f_0)$ and the vertical axis denotes relative values normalized with the driving voltage. For the idealized point scatterer in the far field, the scattering strength is denoted as $s_0\delta(t)$ and the acoustic

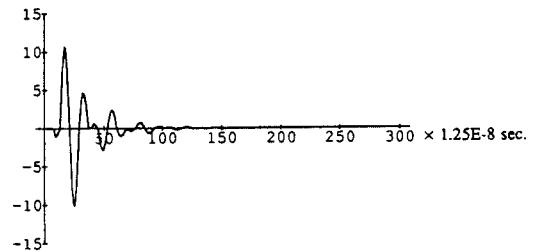


Fig. 9. Transient response of the transmitting transducer

backscattering transfer function $g(R,t)$ in the time domain is derived from the Eqs. 17-19 through some simple arithmetic as

$$g(R,t) = \frac{\rho c s_0 S^2}{8 \pi^2 R^2} \delta'(t - \frac{2R}{c}) \tag{20}$$

where $\delta'(t)$ is a doublet. Figure 10 is the transmitted signal after the convolution with the transfer function. Waveform gets more complicated due to the diffraction, which is undesirable. Figure 11 is the overall time domain response of the dual element transducer. For comparison, the transient waveform in Fig. 9 are directly coupled to the response of the receiving part, and the results are shown in Fig. 12 where the effect of diffraction is not included. Pulse duration time increases a little bit and the waveform gets distorted due to the diffraction. -40dB pulse ring-down time increases from $1.40\ \mu\text{sec}$. to $1.45\ \mu\text{sec}$.

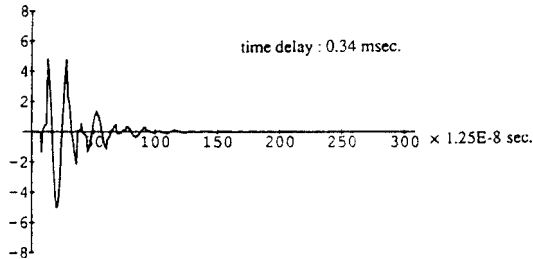


Fig. 10. Transmitted waveform after plying from the transmitting transducer to the target

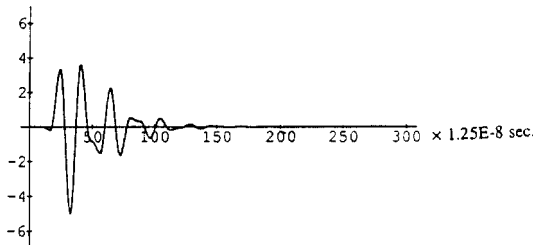


Fig. 11. Overall transient response of the dual element transducer with diffraction

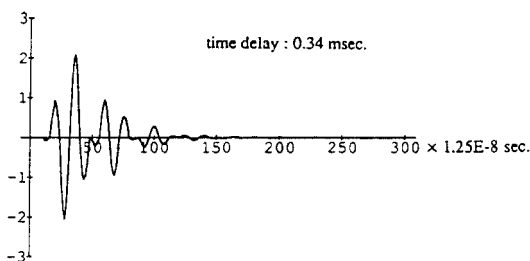


Fig. 12. Overall transient response of the dual element transducer without diffraction

Therefore with the algorithm outlined in Sec. 2, the overall and intermittent responses of the transducer in both the frequency domain and the time domain could be easily calculated and the method could do a more precise performance analysis of NDT transducers.

IV. Conclusion

A theoretical method to analyze ultrasonic transducer performance was developed and was applied to the design of a dual element transducer. The method can check both transmitting and receiving properties of a transducer, and can also reflect the diffraction effect of the loading material in both the frequency and time domains. In the time domain, distinct from the conventional method-inverse transform of frequency domain properties-, the method checks wave interferences at the interface of each material and calculates the transient response in a direct manner without relying on frequency domain results. Further work is under way to elaborate the method so that transducer structures can be optimized once specifications of desired transducer performance are given. Experimental verification of the theoretical results in this study is to be presented in a consecutive paper at a later date.

References

1. W.P. Mason, *Electromechanical transducers and wave filters*, Van Nostrand, Princeton, NJ, U.S.A., 1948.
2. G.Kossoff, *The effects of backing and matching on the performance of piezoelectric ceramic transducers*, IEEE Transactions on Sonics and Ultrasonics, Vol. 13, p.20-30, Mar. 1966.
3. K.E.Sittig, *Transmission parameters of thickness driven piezoelectric transducers arranged in multilayer configurations*, IEEE Transactions on Sonics and Ultrasonics, vol.14, No.1, p.167-174, Oct. 1967.

4. T.M.Reeder and D.K.Winslow, Characteristics of microwave acoustic transducers for volume wave excitation, IEEE Transactions on Microwave Theory and Techniques, vol.17, p.927-941, Nov. 1969.
5. A.D.Pierce, Acoustics-an introduction to its physical principles and applications, Acoustical Society of America, New York, U.S.A., 1989.
6. M.E.Lines and A.M.Glass, Principles and applications of ferroelectrics and related materials, Oxford University Press, London, Great Britain, 1979.
7. V.V.Varadan, private communication.
8. J.H.Goll, The design of broadband fluid loaded ultrasonic transducers, IEEE Transactions on Sonics and Ultrasonics, vol.26, p.385-393, Nov. 1979.

▲ Yongrae Roh



received the B.S. and M.S. degrees in Mineral and Petroleum Engineering from the Seoul National University, Seoul, in 1984 and 1986, respectively. He got the Ph.D. degree in Engineering Science and Mechanics(major in Acoustics) from the Pennsylvania State University, U.S.A., in 1990. He is currently a senior research scientist in the Research Institute of Industrial Science and Technology, Pohang. Major research area includes SAW devices, ultrasonic transducers, and noise & vibration control. He received the 1990 Xerox Award, U.S.A., for the best research in materials.